Heavy and Thermal Oil Recovery Production Mechanisms

Quarterly Technical Progress Report
Reporting Period: April 1 through June 30, 2002

Principal Author: Anthony R. Kovscek
(650)723-1218

Report Date: July 2002

DOE Award Number: DE-FC26-00BC15311

Name and Address of Submitting Organization:

Petroleum Engineering Department
Stanford University
367 Panama Street
Stanford, CA 94305-2220

Disclaimer

Abstract

This technical progress report describes work performed from April 1 through June 30, 2002 , for the project "Heavy and Thermal Oil Recovery Production Mechanisms." We investigate a broad spectrum of topics related to thermal and heavy-oil recovery. Significant results were obtained in the areas of multiphase flow and rock properties, hot-fluid injection, improved primary heavy oil recovery, and reservoir definition. The research tools and techniques used are varied and span from pore-level imaging of multiphase fluid flow to definition of reservoir-scale features through streamline-based history-matching techniques.

Briefly, experiments were conducted to image at the pore level matrix-to-fracture production of oil from a fractured porous medium. This project is ongoing. A simulation studied was completed in the area of recovery processes during steam injection into fractured porous media. We continued to study experimentally heavy-oil production mechanisms from relatively low permeability rocks under conditions of high pressure and high temperature. High temperature significantly increased oil recovery rate and decreased residual oil saturation. Also in the area of imaging production processes in laboratory-scale cores, we use CT to study the process of gas-phase formation during solution gas drive in viscous oils. Results from recent experiments are reported here. Finally, a project was completed that uses the producing water-oil ratio to define reservoir heterogeneity and integrate production history into a reservoir model using streamline properties.

Project Objectives

The objective of this research project is to improve the recovery efficiency from difficult to produce reservoirs including heavy-oil and fractured low permeability systems. This objective is accomplished by developing laboratory techniques and apparatus for studying multiphase flow properties in fractured and unfractured porous media, identifying oil production mechanisms from the pore to the core to field scale, and translating this understanding into mathematical models incorporating newly understood physics.

The project is divided into 5 main areas. These projects and their goals include:

1. Multiphase flow and rock properties—to develop better understanding of the physics of displacement in porous media through experiment and theory. This category includes work on imbibition, flow in fractured media, and the effect of temperature on relative permeability and capillary pressure.

2. Hot fluid injection—to improve the application of nonconventional wells for enhanced oil recovery and elucidate the mechanisms of steamdrive in low permeability, fractured porous media.

3. Mechanisms of primary heavy oil recovery—to develop a mechanistic understanding of so-called "foamy oil" and its associated physical chemistry.

4. In-situ combustion—to evaluate the effect of different reservoir parameters on the insitu combustion process.

5. Reservoir definition—to develop and improve techniques for evaluating formation properties from production information.

Technical progress in each of these areas is now described briefly.

Area 1. Multiphase Flow and Rock Properties

Work in this project area focused on a micro-visual analysis of matrix-to-fracture transfer in transparent, two-dimensional replicas of fractured systems. i.e, micromodels. Most of the progress is associated with establishing the experimental apparatus.

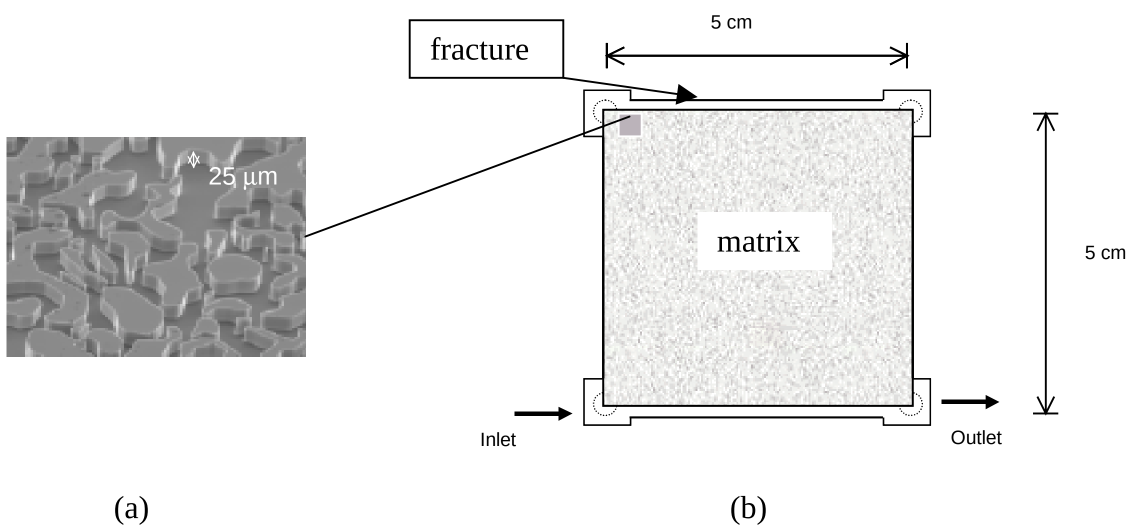

Figure 1. Schematic of the micromodel: The network acts as the porous medium and the adjacent channels act as the high conductivity fractures.

Rationale and Summary–Matrix/Fracture Transfer. Understanding and modeling flow behavior in naturally fractured rocks, including oil and gas reservoirs requires a detailed analysis of these systems at various length scales. The ultimate goal is to provide realistic information on how to model or simulate matrix to fracture transfer under thermal and isothermal conditions. To understand how fluids communicate between the high conductivity fracture and the lower conductivity matrix requires both pore- and core-scale analysis of the problem. The core-scale experimental work is described elsewhere (Rangel-German and Kovscek 2002).

Our recent work at the pore-level is conducted using micromodels where matrix-fracture transfer is visualized through a microscope. Experiments are analogous to those conducted with cores. Etched-silicon-wafer micromodels of the type used by George (1999), initially developed by Hornbrook *et al.* (1991), were used in this work. Typically micromodels are made up of a repeated pattern of an SEM (Scanning Electron Microscopy) image of a reservoir or quarried rock thin section. Usually, digital modification of the image is necessary to ensure continuity in the porous medium. The micromodels here are 5-cm squared etched pore patterns of Berea sandstone. These patterns have grains ranging from the size of 30 to 200 um (Figure 1). The porosity is roughly 0.2 whereas the permeability is approximately 0.1 mD. Two parallel channels etched on either side of the micromodel act as fractures adjacent to the porous medium. Previous progress reports described the design and testing of a micromodel apparatus and holder as well as experiments using water and air (Kovscek 2002).

Further experiments were conducted with oil as the nonwetting fluid. Micromodels were saturated with oil to irreducible water saturation. Water was injected into the fracture at 0.01 cc/min and no water imbibed into the matrix while the fracture was filling. Once the water front reached the end of the fracture, it penetrated into the matrix displacing oil by counter-current imbibition. Fig. 2 shows how the oil is displaced from the matrix to the fracture at discrete locations along the fracture. Oil blobs grow as more oil is pushed into them by the imbibing water. Once the blobs have reached some critical volume they are displaced by the viscous forces in the fracture. This process was found to be intermittent; i.e., a blob grows, it is displaced, and after some time a new blob starts to grow in the same location. However no constant periodicity was found.

These experiments teach that matrix-fracture interaction is controlled by the injection rate; it is apparent that the relative permeability relationships are rate dependent. Wetting and non-wetting fluids will flow simultaneously in both fractures and the matrix, and the combination of these two flow processes results in a combined relative permeability behavior that has not been determined. These experiments help in the understanding of matrix-fracture interaction and are useful while modeling real fracture relative permeability and matrix-fracture transfer functions.

Area 2. Hot Fluid Injection

Work in this project area continued in both experimental and simulation aspects. We are interpreting our high-temperature, high-pressure experiments to understand thermal recovery mechanisms of heavy oil from relatively low permeability rocks. A simulation study was completed to understand thermal production mechanisms of light and medium gravity crude oil during steam injection into diatomite.

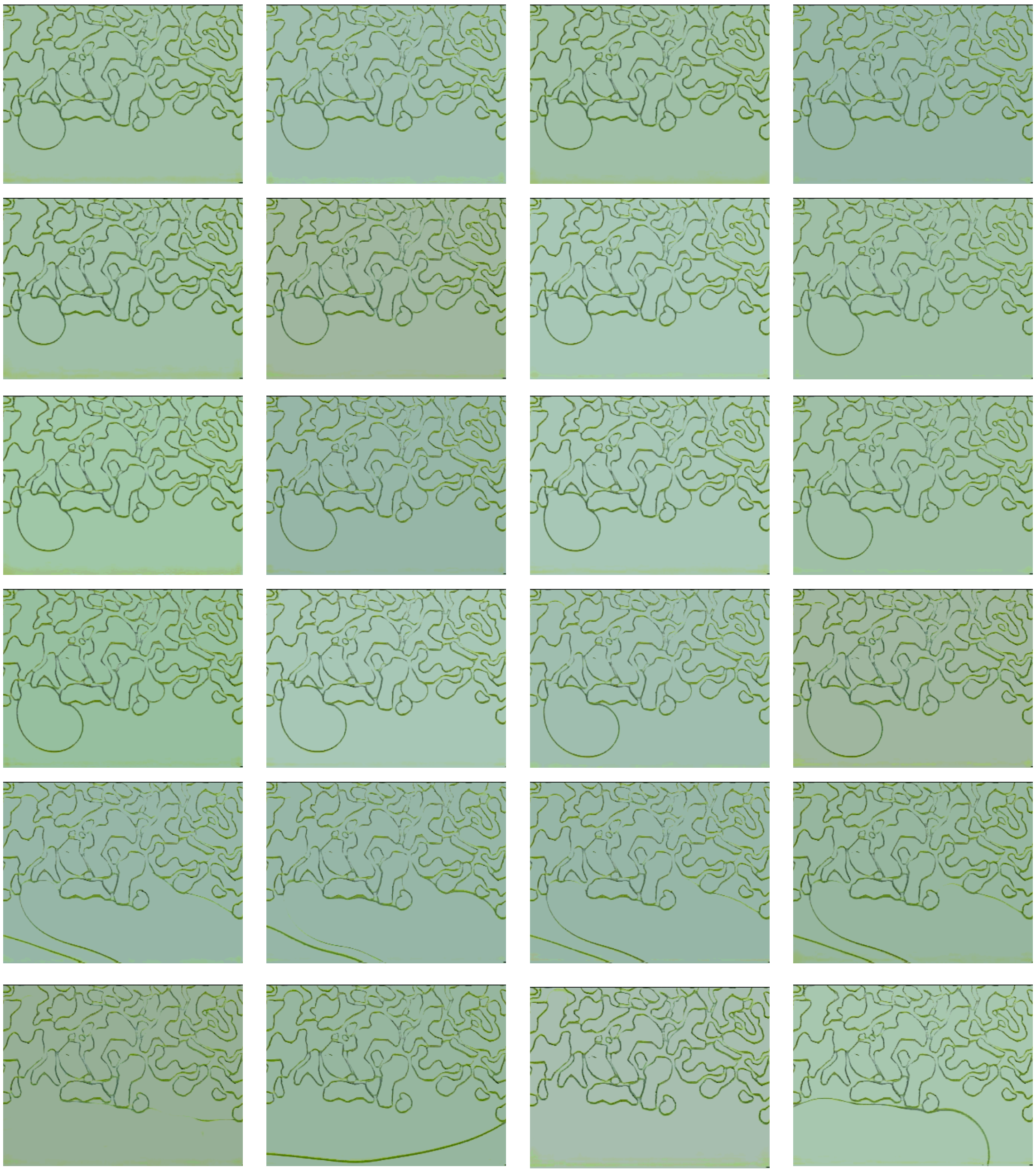

Figure 2. Production of oil by counter-current imbibition of water matrix-fracture interface. Note the growing oil blob on the left in the first images.

Rationale and Summary--Experimental Study of Thermal Recovery. Oil production from many fractured reservoirs is frustrated by not only low matrix permeability but also large oil viscosity and a matrix wettability state that is not sufficiently water wet to favor water imbibition.

As stated previously, thermal recovery using hydraulically fractured wells is one process to improve oil recovery and unlock these heavier resources. Steam injection is typically carried out under saturated conditions and initial heating of a reservoir is accompanied by significant condensation and flow of the resulting hot water away from the injector. Thus, hot-water imbibition is an important component of thermal recovery in fractured, low permeability porous media.

We have performed a series of spontaneous, counter-current water imbibition tests using outcrop diatomite cores (2 to 4 md) and reservoir diatomite cores (0.8 to 2 md). The experiments were isothermal and temperatures from 20 to 180 °C are explored. Decane, two white mineral oils with differing viscosities (35 and 407 cP), and heavy diatomite crude oil were all used as oil phases. At room temperature, oil-phase viscosities ranged from 0.9 to 6400 mPa-s. An X-ray computed tomography (CT) scanner, in combination with a high-temperature and high-pressure core holder, was used to visualize fluid movement and production of these oils. It was observed that temperature has a significant effect on water imbibition rate and residual oil saturation to spontaneous imbibition. In reservoir core filled with crude oil, the spontaneous oil recovery increased from 3% at 40 °C (reservoir temperature) to more than 40% of oil in place at 180 °C. The effect of temperature is to reduce oil-phase viscosity, and we postulate an increase in water wetness of the rock also occurs.

A scaling exercise demonstrated that there are at least two wettability states in the outcrop samples and two lithologies in the reservoir core. However, the degree and importance of change in the wettability state with temperature is not readily demonstrated. For this task, we employ the concept of imbibition potential, Φ_{im}.The potential for a rock to imbibe water is a function of viscosity, interfacial tension, wettability, mobility ratio, and rock properties when gravity is negligible. That is

$$\Phi_{im} = f(f_{\mu r}, f_{\sigma}, f_{w}, f_{r}) \tag{1}$$

where $f_{\mu r}$ is the viscosity ratio function, f_{σ} is an interfacial tension function, f_w is the wettability function, and f_r is the rock-property function. A differentiated form of imbibition potential with regard to temperature is

$$\frac{d\Phi_{im}}{dT} = \frac{\partial\Phi_{im}}{\partial f_{\mu r}}\frac{df_{\mu r}}{dT} + \frac{\partial\Phi_{im}}{\partial f_{\sigma}}\frac{df_{\sigma}}{dT} + \frac{\partial\Phi_{im}}{\partial f_{w}}\frac{df_{w}}{dT} + \frac{\partial\Phi_{im}}{\partial f_{r}}\frac{df_{r}}{dT} \tag{2}$$

where $d\Phi_{im}/dT$, $df_{\mu R}/dT$, df_{σ}/dT, df_w/dT, and df_r/dT are the imbibition potential, viscosity ratio (oil to water), interfacial tension, wettability, and rock-property variation with temperature. These terms are measured independently through experiments. The terms $\partial\Phi_{im}/\partial f_{\mu R}$, $\partial\Phi_{im}/\partial f_{\sigma}$, $\partial\Phi_{im}/\partial f_{w}$, and $\partial\Phi_{im}/\partial f_{r}$ represent the variation of the functionality of imbibition potential with change in viscosity ratio, interfacial tension, wettability, and rock properties. We assume that the imbibition-potential functionality is constant, or is a very weak function of temperature and the fluids employed. The various partial derivatives in Eq. (2) are then constants. The following definitions result: $a_1 = \partial\Phi_{im}/\partial f_{\mu R}$, $a_2 = \partial\Phi_{im}/\partial f_{\sigma}$, $a_3 = \partial\Phi_{im}/\partial f_w$, and $a_4 = \partial\Phi_{im}/\partial f_r$, respectively.

Upon substitution, Eq. (2) reduces to

$$\frac{dP_{im}}{dT} = a_1\frac{df_{\mu r}}{dT} + a_2\frac{df_{\sigma}}{dT} + a_3\frac{df_w}{dT} + a_4\frac{df_r}{dT} \tag{3}$$

When the factors, a_1, a_2, a_3 and a_4 are determined experimentally, or theoretically, the imbibition potential is predicted at different temperatures through integration of Eq. (3).

From experiments and physical data for the fluids employed, we obtained $d\Phi_{im}/dT$, $df_{\mu R}/dT$, and df_{σ}/dT functions. However, the contact angle variation with temperature for water/oil/diatomite is currently unknown. Diatomite is a siliceous rock; therefore, we employed the contact angle versus temperature relationship measured for water/mineral oils/quartz systems by McCaffery to determine the df_w/dT function for outcrop/water/decane. The term df_r/dT is set to 0, because the experimental apparatus is designed to maintain a constant net confining stress regardless of temperature, and, accordingly, the effect of temperature on porosity and permeability is negligible.

Equation (3) is reduced to three terms with weight factors. By regressing $d\Phi_{im}/dT$, $df_{\mu R}/dT$, df_{σ}/dT, and df_w/dT at three different temperatures for the diatomite/water/decane system, the weight factors a_1, a_2, and a_3 are determined. It was assumed that the measured weight factors do not change with temperature and are valid for all water/oil/diatomite systems in this study. This assumption is verified *a posteriori*.

One of the important implications of Eq. (3) is to identify wettability alteration with temperature. The terms $d\Phi_{im}/dT$, $df_{\mu R}/dT$, and df_{σ}/dT are obtained through water imbibition tests for various measured viscosity ratios and interfacial tension. The sole unknown effect is that of wettability. If df_w/dT is greater than 0 at a given temperature, wettability alteration occurs with an increase in temperature. The Φ_{im} versus T data shown collected experimentally are matched versus temperature for the water/Blandol, water/ PAO40, and water/crude oil systems by adjusting the df_w/dT function. For simplicity, a linear relationship is assumed:

$$\frac{df_w}{dT} = mT + b \tag{4}$$

Figure 3 displays the results of this exercise for the various experiments in outcrop core. All views in Fig. 3 present the variation in imbibition potential with wettability alteration included as a solid line. Results when wettability alteration is not accounted for (i.e., $df_w/dT = 0$) are given as dashed lines. Experimental data are given as symbols. For water/decane the temperature range of interest is 22 to 88 °C. For the remaining systems, the temperature range of interest is 40 to

180 °C. All experiments in outcrop core exhibit some shift toward increased water wetness as temperature increases. Recovery increased from 12 to 30 % as a function of temperature for the various fluid systems used. The effect is likewise considerable when crude oil is used as the nonwetting fluid.

The analysis summarized in Fig. 3 assumed that the coefficients a_1, a_2, and a_3 were constant and independent of the fluids within the core. Constancy of these coefficients across all fluid systems was checked. Numerical averages and the variation of each coefficient are $a_1 = 8.7 \times 10^{-6} \pm 0.03 \times 10^{-6}$ cP^{-1}-$min^{-0.5}$, $a_2 = -5.69 \times 10^{-4}$ cm/dyne-$min^{0.5} \pm 0.16 \times 10^{-4}$, and $a_3 = 0.0168 \pm 0.0008$ $min^{-0.5}$. Within experimental error, these values are identical to the prior values of a_1, a_2, and a_3. The assumption of invariant coefficients is self consistent.

Our future work in this area will delineate a mechanism for this wettability change and improvement in recovery performance.

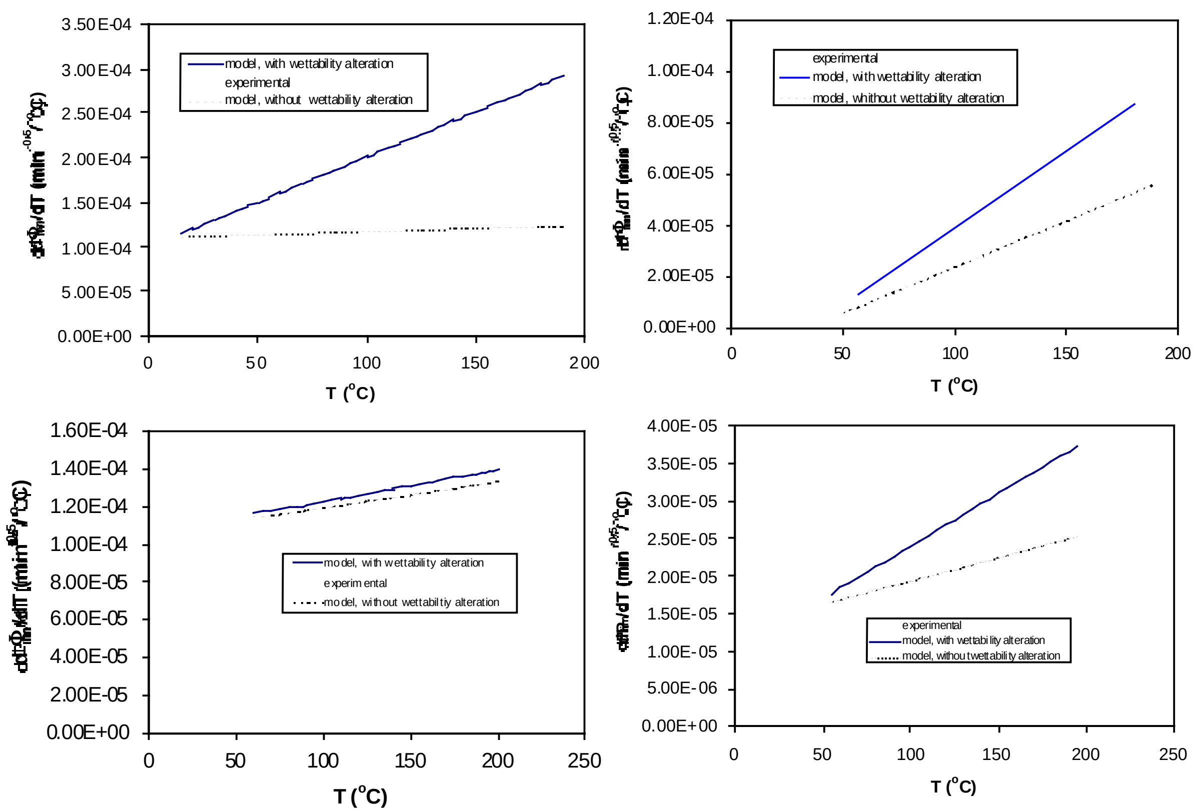

Figure 3. Effect of temperature on imbibition potential for water imbibition in oil saturated diatomite core: upper left–decane, lower left–PAO40, upper right–kaydol, lower right–crude oil.

Rationale and Summary--Simulation Study of Thermal Recovery Mechanisms. The purpose of this study is to improve our understanding of the mechanisms of steam drive in low permeability fractured reservoirs containing lighter oils. Steam injection into heavy oils has been characterized very well over the last 40 years, but the light oil process is much less understood, especially with regard to the relative importance of mechanisms.

A pattern reservoir simulation study of steam injection into a hydraulically-fractured diatomite formation has been completed. A paper is in preparation, and so only a summary is given here. The information gained includes a better understanding of the recovery efficiencies, primary recovery mechanisms, and in-situ saturation and hydrocarbon composition profiles in steam drives. Multiple reservoir descriptions varied from homogeneous to quite heterogeneous. Viscosity, relative permeability, oil-phase composition, and other rock and fluid properties are realistic and come from a prior field study.

Comparison among steamflood and waterflood results show that the incremental recovery ranges from about 15% up to around 35% of initial oil in place. The distribution of permeability is a key factor in determining incremental recovery. As permeability becomes more correlated in a direction roughly parallel to pattern boundaries, recovery decreases. On the other hand, a highly variable, but uncorrelated, permeability distribution displays good recovery. Regardless of the distribution of permeability, it is apparent that steamflooding heterogeneous, low permeability, hydraulically-fractured systems significantly increases the recovery as compared to waterfloods. It is likely that the recovery from low permeability naturally fractured reservoir can be improved similarly using steam injection. These candidates suffer from the same problems as diatomites, such as below average primary recovery and poor waterflood performance

For the reservoir and fluid descriptions employed, thermal expansion accounts for one- half to two-thirds of the incremental recovery early in the injection life, that is, until the cold water bank breaks through. Results vary with fracture length, the reservoir description, and the shape of relative permeability functions. After breakthrough, vaporization, viscosity reduction, and thermal expansion all contribute approximately equal amounts to the recovery. At late times and as the distillate bank approaches the producer, vaporization becomes the most important recovery mechanism.

A clearly differentiable distillate bank does not form. Instead there is a bank of distilled, condensed hydrocarbons and hot water. It is characterized by the lightest hydrocarbon component farthest downstream and grades to heavier components at its rear. The mixed distillate-hot-water bank is preceded by a cold water bank and followed by the steam front.

Area 3. Mechanisms of Primary Heavy Oil Recovery

This project area is concerned with so-called foamy oil production. More correctly this process is characterized as heavy-oil solution gas drive. Gas released from solution during pressure depletion remains dispersed rather than uniting to form a single phase.

Rationale and Summary--Solution Gas Drive in Viscous Oils. Primary production in some heavy-oil reservoirs is larger than that estimated by conventional calculations. Conventionally, the main driving force behind primary recovery is pressure depletion through solution gas drive. Solution gas drive is the mechanism, whereby the lowering of reservoir pressure through production in an undersaturated reservoir reaches the bubble point where gas starts to evolve from solution. The evolved gas does not begin to flow until the critical gas saturation has been reached. Once the critical gas saturation point is reached, there is an increase in rate of pressure drop due to the production of the gas-phase. It has been noted that the oil at the wellhead of these heavy-oil reservoirs resembles the form of foam, hence the term “foamy oil”. A key to developing a mechanistic understanding of heavy-oil solution gas drive is to delineate bubble growth, interaction and gas flow experimentally.

The equipment is setup as in Fig. 4. The sandpack holder is 16 inches long, 2 inches in diameter, and has 11 pressure ports attached to it. A circular water jacket surrounds the sandpack holder thus allowing for experiments to be conducted at a specified temperature. The water jacket also helps to improve images obtained by X-ray computed tomography (CT). The pressure ports are connected using high pressure plastic tubing (EFTE) to a 12 port multiplexer (Scannivalve 12L8-175), that leads to a central pressure transducer (Scannivalve). This system is hooked up to a computer via the digital interface unit (Scannivalve) where automatic remote port measurements are recorded using a visual basic program. The position of the pressure ports is such that they do not interfere with axial CT scans of the sandpack. The CT scanner is a Picker 1200 SX X-ray scanner and the sandpack is scanned lengthwise. A high pressure piston accumulator with holding capacity of 882 mL is used to combine the CO_2 with dead oil. An ISCO Model 500D syringe pump is used in conjunction with an accumulator. This accumulator is filled with water and is used at the outlet as an intermediary oil depletion device. This setup allows us to conduct constant volumetric depletion at a set rate.

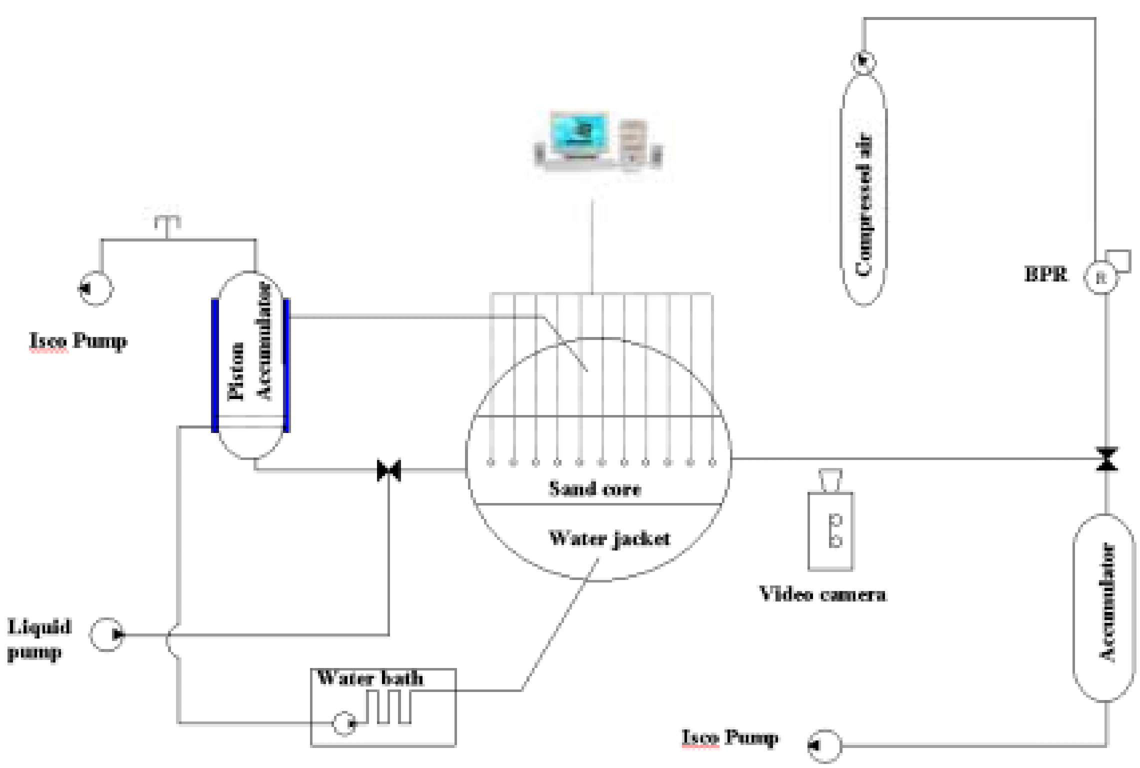

Figure 4. Apparatus for viscous-oil solution gas drive experiments.

Experiments are ongoing. Figure 5 displays the average sandpack pressure as function of the volume expanded. The curves exhibit characteristic rapid pressure decline in the single-phase region that ends in a minimum and slight rebound of system pressure as gas evolves from the oil. Once gas and oil phases are present in the core, the system compressibility is high and the rate of pressure decline is much less. The evolution of gas saturation was imaged in-situ via X-ray CT scanning. Figure 6 displays a typical image. White represents a gas saturation of 100% whereas black represents 0% gas saturation. The elapsed time is given in hours:minutes:seconds format below each image. The production end is on the left whereas the closed end of the core lies on the right. Gas evolves first near the outlet and the progressively toward the right.

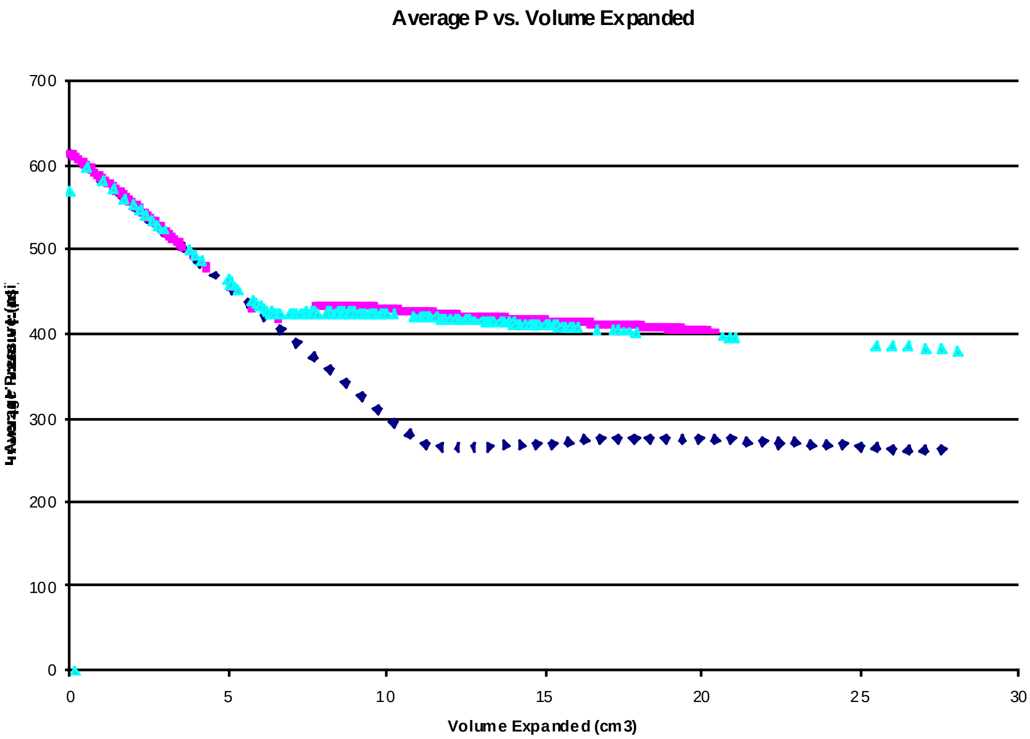

Figure 5 – Average pressure vs. volume expanded.

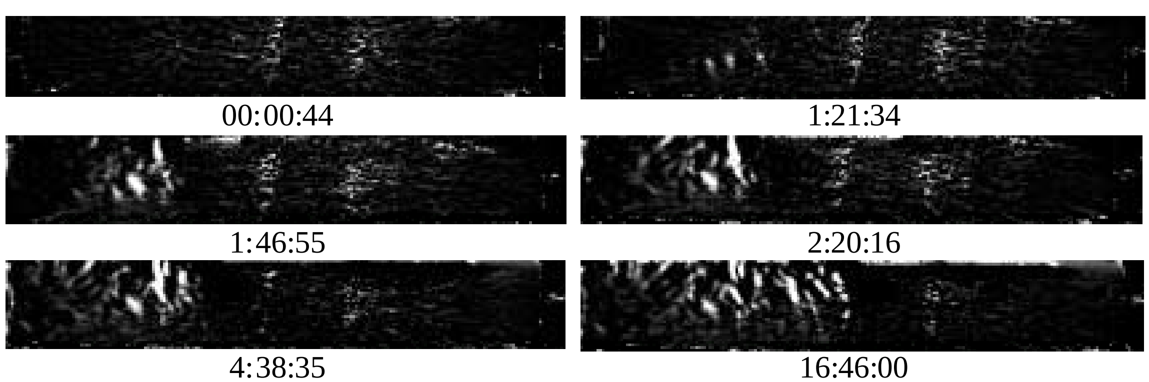

Figure 6. Evolution of gas saturation in sandpack: mineral oil (220 cp) and carbon dioxide. White shading corresponds to gas and black to oil. Depletion rate is 0.16 ml/min.

When complete, we will have a much clearer picture of the formation of gas phase and how nucleated bubbles unite to become a single phase as time evolves. This information will be garnered as a function of depletion rate, oil viscosity, and a comparison among crude oil and mineral oil will be made.

Area 4. In-Situ Combustion

Two tasks are underway in this area. The first is the preparation of a Chapter for the Reservoir Engineering Section of the Petroleum Engineers Handbook detailing material and energy balance calculations that can be used to design an in-situ combustion field project. It has been accepted and will appear in 2003. The second task regards the potential for in-situ upgrading during combustion.

Rationale and Summary--In-Situ Upgrading. Crude oil upgrading is of major economic importance. Heavy crude oils exist in large quantities in the western hemisphere but are difficult to produce and transport because of their high viscosity. Some crude oils contain compounds such as sulfur and/or heavy metals causing extra refining problems and costs. In-situ upgrading could be a beneficial process. For heavy oils, numerous field observations shown upgrading of 2 to 6 °API for heavy oils undergoing combustion (Ramey, 1992) . During in-situ combustion of heavy oils, temperatures of up to 700°C can be observed at the combustion front. This is sufficient to promote some upgrading. This task examine the changes caused by the various reactions occurring during combustion with emphasis on the upgrading potential for various oil types. Secondly, combustion-tube runs aimed at sulfur removal are conducted.

Sulfur can be a major problem for refiners. To investigate the possible use of in-situ combustion to improve sulfur content of produced oil three combustion tube runs were performed using a matrix made of 95% Ottawa sand and 5% fire clay. All three runs were made using a crude oil containing 6% by weight sulfur. In the runs, oil saturation was about 20% and water saturation about 20%. The oil, water and matrix were premixed and packed in the combustion tube. The first run was a simple dry forward combustion run. As the combustion was not good, we decided to use metallic additives. The second run was made using a solution of 5% by weight of stannous chloride in the water to increase the amount of fuel deposited. The third run contained 5% iron nitrate in the water.

As the behavior of both runs with metallic additive was similar, we will only detail the results of the run where tin chloride was used. The temperature profiles as a function of time are shown in Fig. 7. The average front temperature was about 500°C. This represents an increase of about 50°C over the run without additive. Figure 8 shows the produced gas composition. The combustion was stable with only minor fluctuations. Almost all of the oxygen injected was consumed. Fuel concentration (Fig. 9) was also stable at a value around 0.04 grams per cubic centimeter of the pack. This run was stopped after four hours because a leak developed.

The run with iron nitrate was made after repairing the leak and the results were similar to the run made with tin chloride. For the sake of brevity the figures showing temperatures, gas compositions and fuel concentration are omitted. In both cases with metallic additives, the amount of sulfur in the produced oil was reduced to less than 1% by weight from the original 6%.

Although it was necessary to use metallic additives to promote fuel deposition and obtain a good burn and oxygen utilization of this light oil, sulfur removal by in-situ combustion appears promising. We can also postulate that heavy metals, sometimes present in the oil, can be removed and left behind in the reservoir in a similar manner. In the field, some of the oil will be moved to the producer without experiencing the high temperature at the front but will be displaced by the steam ahead and undergo some distillation. The portion of the oil burnt as fuel is the heavy residue and contains the unwanted products. This type of catalytic process appears to be especially valid for heavy oils (Moore *et al.*, 1999).

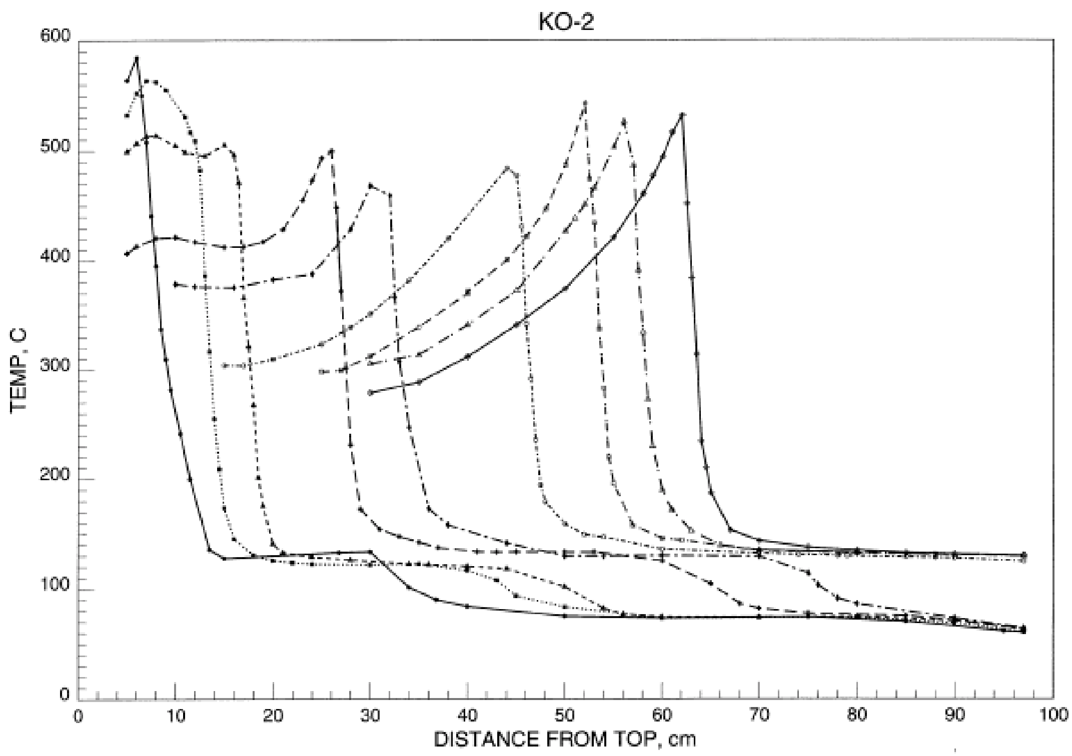

Fig. 7. Temperature profiles, with 5% $SnCl_2$ solution.

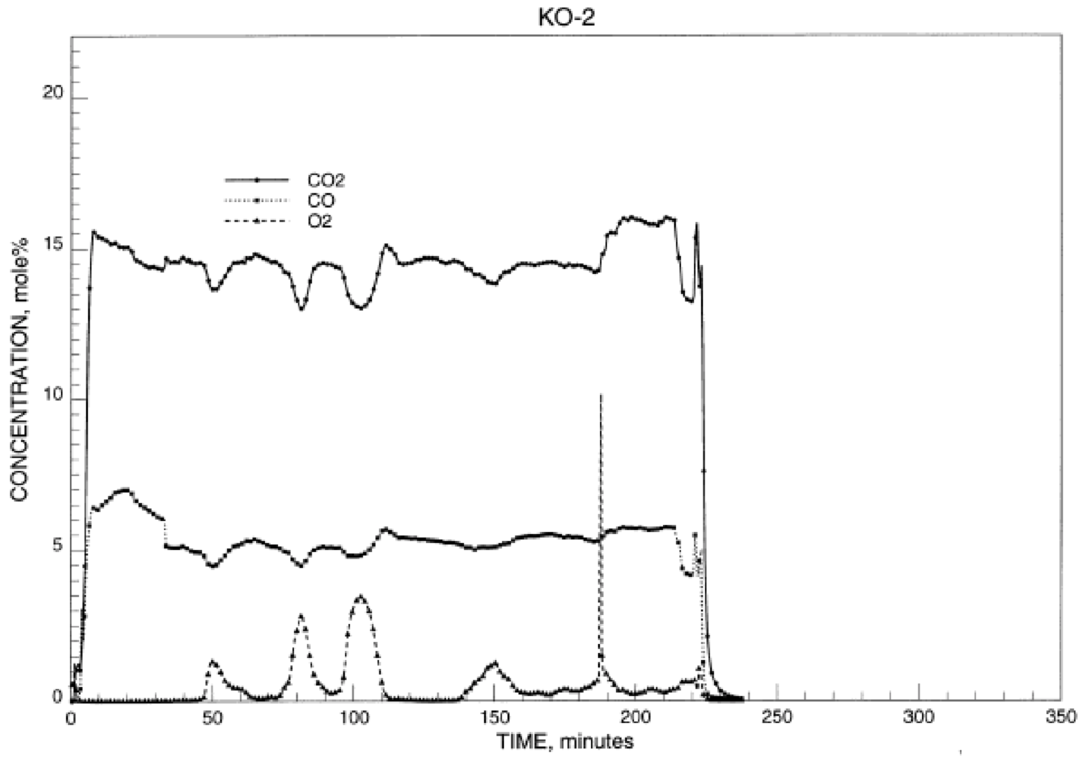

Figure 8. Effluent gas composition, with 5% $SnCl_2$ solution.

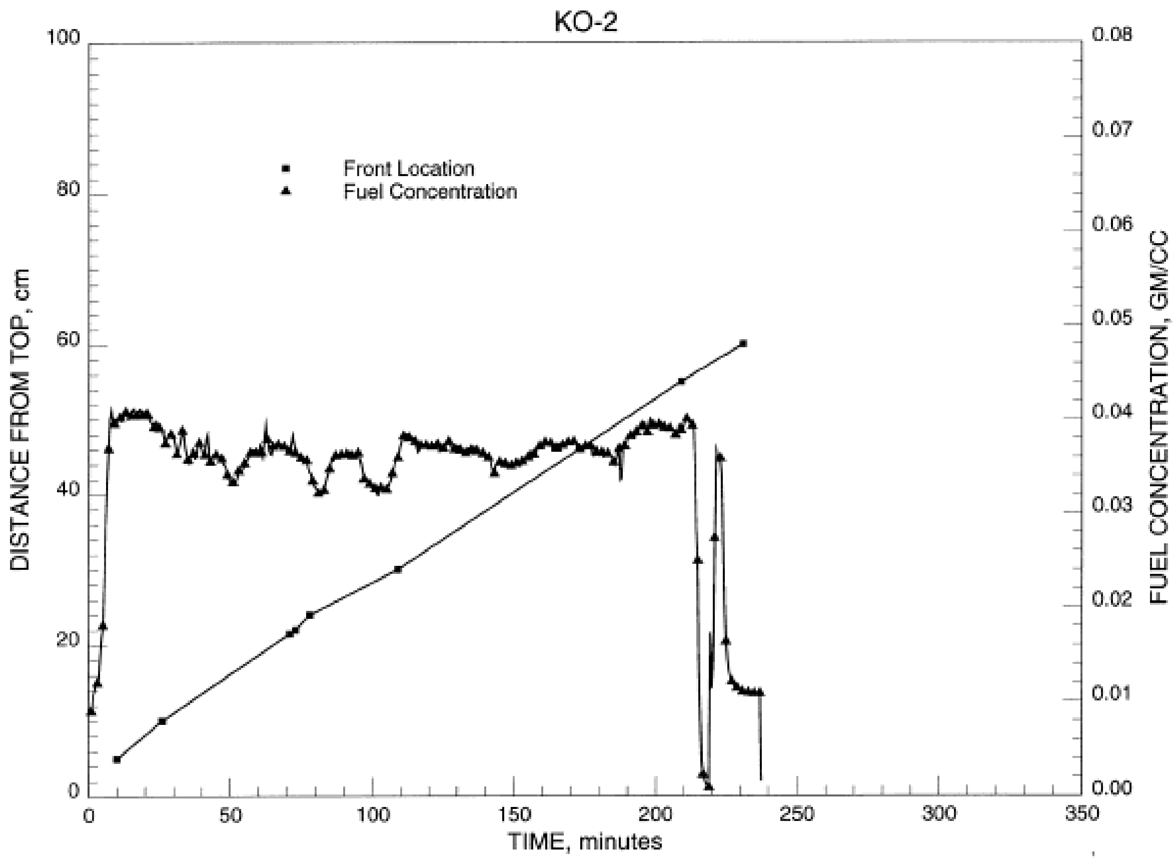

Fig. 9. Front location and fuel concentration, with 5% $SnCl_2$ solution.

Area 5. Reservoir Definition.

Reservoir definition is the process of using data from a variety of length scales (pore-core-reservoir) and sources (laboratory-field) to improve our understanding of reservoirs and their petrophysical properties. Work during the past quarter focused on developing a technique that integrates production history into reservoir models using streamline-based properties.

Rationale and Summary--Streamline-Based Time-of-Flight Ranking. The reservoir models generated by geostatistical techniques provide equally probable reservoir descriptions that honor observed geology. However, flow simulation results on these models may vary widely indicating uncertainty. Constraining geostatistical models to known production history reduces uncertainty. To this end, we have developed a streamline-based algorithm for ranking geostatistical realizations with regard to production history. A paper has been prepared and submitted for publication (Wang and Kovscek, 2002); hence, only a summary is given here. First, a rapid, streamline-based inversion method (Wang and Kovscek 2000) or any other inversion method is applied to obtain a history-matched reservoir model. Then, unit mobility ratio streamline geometries are computed, without full flow simulation, for the history-matched model and the geostatistical models considered. Each model is then compared to the history-matched model with regard to streamline properties, such as time-of-flight. In this way, a reservoir model that matches production history and honors known geological information is obtained. The use of full flow simulation is minimized.

This method is based on the observation that there is approximately a linear correlation between unit mobility ratio streamline properties and nonunit mobility ratio reservoir flow simulation results, under appropriate assumptions. The streamline time-of-flight cumulative distribution function indicates the connectivity between injector-producer pairs, and consequently it is characteristic of flow simulation results regardless of mobility ratio. Exhaustive flow simulation and theoretical derivation established correlation among the following data pairs: 1) streamline *TOF cdf* and producer water cut, 2) unit mobility flow-rate at one time value and that in comprehensive flow simulation, and 3) N_p^E and N_p. With these data pairs, reservoir models ranked in terms of streamline properties are also ranked in terms of their match to the observed production history. Computation of streamline geometries and properties is computationally efficient. The computational effort per reservoir model is equivalent to one time-step of an IMPES flow simulation.

The ranking method requires that a history-matched model be obtained first. The history match does not necessarily need to be constrained to geology. Then, geostatistically consistent models are generated and compared to the history-matched model with regard to streamline properties. A subset of models with tolerable mismatch are selected to run flow simulation and thereby verify that they match the observed behavior. In this manner, multiple models are obtained that reproduce satisfactorily production history and are constrained to geological information. An exercise demonstrated that partial production history when used in combination with streamline-based ranking reduced significantly the uncertainty of forecasting reservoir performance.

The ranking results do not depend on the history-matching method or the initial reservoir model, but depend on the accuracy of the match used to obtain the target *TOF cdf*. Additionally, there is no restriction that the reservoir models must have the same grid-block dimensions as the history-matched model. Therefore, fine-grid models with a million cells can be ranked and selected efficiently when history matching is performed on a coarse grid. This provides an efficient way to downscale history-matched models.

References

Batycky, R. P., Blunt, M. J., and Thiele, M. R.: “A 3D Field-Scale Streamline-Based Reservoir Simulator,” *SPE Reservoir Engineering*, (November 1997) pp. 246-254.

Deutsch, C. V. and Journel, A. G.: GSLIB, Geostatistical Software Library and User’s Guide, Second Edition, Oxford University Press, New York (1998).

George, D.S.: “Visualization of solution gas drive in viscous oil,” M. S. Thesis, Stanford University (September 1999).

Hornbrook, J.W., Castanier, L.M. and Pettit, P.A.: “Observation of foam/oil interactions in a new, high-resolution micromodel,” SPE 22631, paper presented at the 66th Annual Technical Conference and Exhibition of the SPE, Dallas (October 6-9, 1991).

Kovscek, A. R. "Heavy Oil and Thermal Oil Recovery Production Mechanisms, Quarterly Technical Progress Report" (2002).

McCaffery, F. G. "Measurement of Interfacial Tensions and Contact Angles at High Temperature and Pressure". *Journal of Canadian Petroleum Technology*, July-Sept. (1972) pp. 26-32.

Moore, R. G., Laureshen, C.J.,Mehta, S.A., Belgrave, J., Ursenbach, M, Weissman, J. and Kessler, R., "A Downhole Catalytic Upgrading Process for Heavy Oil Using In-Situ Combustion," *Journal of Canadian Petroleum Technology* 38 (13) (1999).

Ramey, H.J., Jr, Stamp, V.V., Pebdani, F.N.. "Case History of South Belridge, California, In-Situ Combustion Oil Recovery," SPE 24200, Proc. 9th SPE/DOE EOR Symposium, Tulsa, (April 21-24, 1992).

Rangel-German, E. and Kovscek, A.: "Experimental and Analytical Study of Multidimensional Imbibition in Fractured Porous Media," *Journal of Petroleum Science and Engineering*, 36(1-2), (2002) pp. 45-60.

Wang, Y. and Kovscek, A. R. : "Streamline Approach for History Matching Production Data," *SPE Journal* , October (2002). pp. 353-362 .

Wang, Y. and Kovscek, A. R. : "Integrating Production History into Reservoir Models Using Streamline Time-of-Flight Ranking," *Petroleum Geoscience* (submitted June 2002).